Journal of Structural Chemistry. Vol. 54, No. 2, pp. 332-340, 2013

POLYTETRAHEDRAL ORDER AND CHEMICAL SHORT-RANGE ORDER IN METALLIC MELTS

© **A. S. Roik,[1] A. V. Anikeenko,[2] and N. N. Medvedev[2,3]**

UDC 539.266:538.214

The reasons are investigated for the prepeak and the asymmetry of the second peak in the structure factor curve that are observed in a variety of metallic melts. The prepeak is observed as an additional maximum in the left wing of the main peak of the structure factor for multicomponent melts and is attributed to their chemical short-range order (CSRO). The asymmetry of the second peak in the structure factor, which is usually explained by the "icosahedral" (polytetrahedral) order in the melt, is observed both for multicomponent systems and for pure metals. However, some aluminum alloys with transition metals exhibit the two features simultaneously, which requires an explanation. An X-ray diffraction study of the liquid ternary $Al_{66.6}Mn_{16.7}Co_{16.7}$ alloy is performed at 1393 K and that of liquid copper at 1353 K, 1403 K, and 1553 K. The reverse Monte Carlo (RMC) method is used to derive structural models of these and other melts. Structural analysis of these melts is conducted using Delaunay simplices. A theoretical simulation of CSRO is performed in the model of liquid aluminum, the structure factor of which does not have these features. It is discussed that CSRO can exist in a melt regardless of the presence of the polytetrahedral order.

DOI: 10.1134/S002247661302008X

Keywords: metallic melts, single-crystal X-ray diffraction analysis, prepeak, icosahedral short-range order, chemical short-range order, polytetrahedral clusters.

INTRODUCTION

The possibility of producing quasi-crystalline phases by quenching from metallic melts arouses interest in the structure of equilibrium and supercooled aluminum melts with transition metals, which tend to form these phases [1, 2]. With the growth in the number of components, it is increasingly difficult to analyze the diffraction data and interpret the structure of the melt; therefore, computer simulation is widely used in addition to XRD experiments. Analysis of the structural models of the melt gives additional information on the partial characteristics and local structure.

The characteristic feature of the structure factor (SF) curves of metallic melts is the presence of a *prepeak* (an additional maximum (shoulder) at small values of the diffraction vector) and an *asymmetric second peak.* The prepeak is believed to be caused by the presence of a medium-range order in the system, i.e., a structural organization of atoms beyond the nearest coordination sphere [3]. In other words, the prepeak is observed when the system has a characteristic length scale exceeding the size of the atoms [4, 5]. The prepeak can be easily obtained in a model system by giving it a new length scale. For example, it was shown in [6, 7] that the removal of a part of atoms from a homogeneous disordered packing according

[1]Chemistry Department, National Taras Shevchenko University of Kyiv, Kyiv, Ukraine; sasha78@univ.kiev.ua. [2]Institute of Chemical Kinetics and Combustion, Siberian Division, Russian Academy of Sciences, Novosibirsk, Russia. [3]Novosibirsk State University, Novosibirsk, Russia. Translated from *Zhurnal Strukturnoi Khimii*, Vol. 54, No. 2, pp. 269-277, March-April, 2013. Original article submitted May 22, 2012.

to a given pattern leads to a sharp prepeak in the SF. The position of the prepeak can be varied by changing the length scale in the pattern.

In real systems, the medium-range order arises in multicomponent systems owing to specific interactions between the components. For example, melts of alkaline metals with elements of group IV and V (Sn, Sb, and Pb) contain tetrahedral and more complex polyanionic structures with covalently bonded chains of atoms surrounded by alkali metal ions [8]. All this explains the existence of correlations in the arrangement of atoms at medium scales and, consequently, leads to a prepeak in the experimental SF. Since these correlations arise from chemical interactions between the atoms, we can say that the reason for the prepeak is the "chemical order." There are two aspects of this order. First, it can lead to the appearance of structural features in the system, e.g., a geometrically expressed length scale greater than the nearest interatomic distances. On the other hand, if the concentration of atoms of one component around another is different from the stoichiometry in a melt, which is referred to in the literature as *chemical short-range order* (CSRO) [9, 10], then the difference in the scattering power of the components may lead to a prepeak in the SF curves. In this paper we show that such an order can be created in a homogeneous fluid model without affecting the geometric structure of the melt.

The asymmetry of the second peak of the SF is usually attributed to the *icosahedral short-range order* (ISRO) [1, 11, 12]. The icosahedron, as an element of the structure of liquids, was proposed by Frank [13] to explain the supercooling of liquids and has been used in many studies so far. However, this idea gives a simplified understanding of the structure of liquids. Recall that the icosahedron can be understood as a shell consisting of 12 atoms around the central atom. Together with the central atom, they form 20 tetrahedra whose shape is close to perfect. In other words, the central atom draws together a cluster of 20 tetrahedra around itself. However, these tetrahedra are able to join together differently, forming linear and branched clusters, five-membered rings, and their many different combinations. All the interatomic distances found in the icosahedron, which manifest the structure factor, are also found in polytetrahedra. Therefore, it is more correct to speak about a *polytetrahedral order* (PTO) in these systems [14, 15]. Unlike the prepeak, the asymmetry of the second maximum in the SF is often observed for pure metals. Almost all liquid transition metals [11, 12, 16, 17] exhibit the asymmetry at temperatures close to the liquidus line and in the supercooled state. On the other hand, some metals, e.g., aluminum, have no features in the SF over a wide temperature range. In the case of liquid copper, there is published experimental evidence for the absence of asymmetry of the second maximum [18] whereas computer simulation shows its presence [19]. In this paper we carry out an XRD study and simulation of liquid copper at different temperatures. It is shown that the asymmetry of the second maximum appears simultaneously with the strengthening of the polytetrahedral order at lower temperatures.

The simultaneous presence of the prepeak and asymmetric second peak in the SF of aluminum alloys ($x_{Al} > 50\%$) with transition metals can be interpreted as a simultaneous presence of the polytetrahedral order and CSRO. It remains unclear how these types of ordering interact in the formation of short- and medium-range order. It is suggested in [20] for the liquid $Ni_{20}Al_{80}$ alloy that it contains distorted icosahedra, which, by touching each other, form aggregates of a typical size of 0.5-2 nm. The authors [20] conclude that it is the icosahedral order that adds a new length scale to the system. On the other hand, the authors of [21, 1] propose to reconcile the icosahedral order in the melt with the presence of the CSRO due to the formation of the icosahedral shells of aluminum atoms around the transition metal atoms whose size is smaller than that of aluminum.

To investigate the relationship between the polytetrahedral order and CSRO, we carried out an XRD study and simulation of the structure of the liquid $Al_{66.6}Mn_{16.7}Co_{16.7}$ alloy at 1393 K, which corresponds to the crystalline Al_4MnCo compound [22]. We also conduct the simulation and analysis of the structure of liquid Al, Co, Cu, and the liquid $Al_{76.5}Co_{23.5}$ alloy using the previously obtained diffraction data.

MATERIALS AND EXPERIMENT

The ternary $Al_{66.6}Mn_{16.7}Co_{16.7}$ alloy was prepared from high purity Al (A999 grade) and electrolytic Mn (99.6 wt.%) and Co (99.8 wt.%) by melting the components in a KPTM-2 electric arc furnace with a nonconsumable tungsten electrode in an atmosphere of purified argon. The diffraction study of the single-component liquid metal used electrolytic copper

(99.8 wt.%). Experimental measurements were carried out in an atmosphere of purified helium. Liquid copper was studied at 1353±5 K (m.p.), 1403 K (m.p. + 50 K), and 1553 K (m.p. + 200 K), and the liquid $Al_{66.6}Mn_{16.7}Co_{16.7}$ alloy was studied at 1393 K (m.p. + 50 K).

The intensity curves (ICs) of X-rays scattered from the free surface of the melt were obtained with a θ–θ-diffractometer using MoK_α radiation (λ = 0.071069 nm), which was monochromatized by a pair of differential filters of ZrO_2 and Y_2O_3. The diffractometer and the methodology of the high-temperature XRD experiment are described in [23]. The experimental intensity curves were processed with regard to the corrections for polarization and angular dependence of incoherent scattering [24]. The normalization of the intensity curves was based on the Weinstein equation with atomic factors corrected for anomalous dispersion [25]. The calculation of the SF ($a(S)$ curves) and radial distribution function ($g(r)$) was performed by the method described in [23].

SIMULATION AND METHODS

The computer models of liquid Al at 973 K, Co (1803 K), and Cu (1353 K, 1403 K, and 1553 K) and liquid binary $Al_{76.5}Co_{23.5}$ (1393 K) and ternary $Al_{66.6}Mn_{16.7}Co_{16.7}$ (1393 K) alloys were generated using the reverse Monte Carlo (RMC) method [26] from the experimental data obtained in [27] and in this study. Each model contains 10^4 atoms of the stoichiometric composition in a model box with periodic boundary conditions. In generating the models, we used the experimental melt densities and the distances of closest approach between atoms: σ_{AlAl} = 0.235 nm, σ_{TMTM} = 0.21 nm, and σ_{AlTM} = 0.21 nm. Seven independent models were generated for each system and used for the averaging of the calculated parameters. In the case of the ternary melt, the atomic scattering factors of the transition metals are rather close, which makes it impossible to correctly distinguish their partial contributions. Therefore, in the analysis of the structural models, the Co and Mn atoms in the liquid ternary $Al_{66.6}Mn_{16.7}Co_{16.7}$ alloy were treated as one type of atoms (TM).

The local structure of the melts was analyzed by the Voronoi–Delaunay method [28]. Each model configuration was split into Delaunay simplices (DSs), i.e., groups of four geometrically neighboring atoms. After that their patterns were analyzed. A characteristic property of all simple liquids, metallic melts, and disordered packings of identical spheres [29, 30, 15, 31] is the presence of a large number of DSs whose shape is close to that of a regular tetrahedron. For a quantitative analysis of the shape, we used a measure T, which is quite simple and is used in various studies to identify the class of tetrahedral atom configurations [30]

$$T = \frac{1}{15 l_0^2} \sum_{i \neq j} (l_i - l_j)^2, \quad (1)$$

where l_i and l_j are the lengths of the edges of the simplex and l_0 is the average length of the edges. For a perfect tetrahedron, the measure T is zero; this value increases with increasing distortion of the simplex. The threshold value of T for DSs regarded as good tetrahedra was chosen to be 0.018. It was derived by the calibration of T with the use of a perturbed fcc crystal [30]. Below, the Delaunay simplices with $T < 0.018$ will be called *quasi-perfect.*

EXPERIMENTAL DATA

Fig. 1 shows the experimental curves of the structure factor of liquid copper at 1353 K, 1403 K, and 1553 K. It is evident that, at temperatures close to the melting point, the second peak is asymmetric, becoming more symmetric with increasing temperature (inset in Fig. 1). It may be noted that the intensities of all the SF peaks are observed to increase with decreasing temperature. The strengthening of oscillations is also observed in the radial distribution function (RDF). Note that over the temperature range used in the study (1353 K to 1553 K), the most likely shortest distance in liquid Cu is constant at 0.250±0.001 nm.

The experimental and model (calculated by the structural model) SFs of the liquid $Al_{66.6}Mn_{16.7}Co_{16.7}$ alloy at 1393 K are shown in Fig. 2. The figure shows a good agreement of the curves, including near the prepeak and at the second

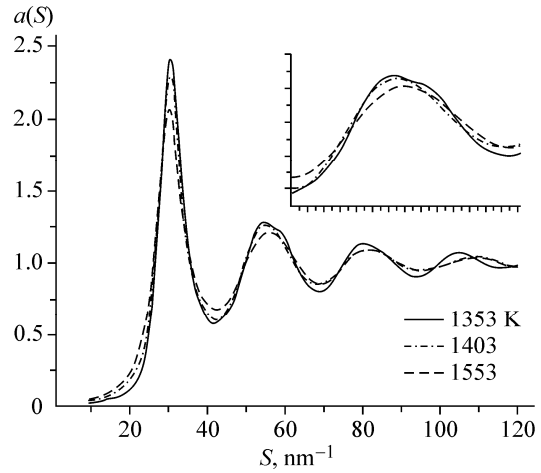

Fig. 1. Experimental curves of the structure factor of liquid copper at different temperatures. The inset is an enlarged view of the second peak.

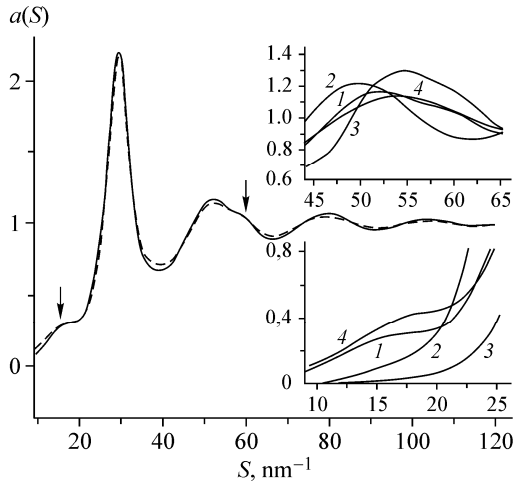

Fig. 2. Experimental (solid line) curve of the structure factor of the liquid $Al_{66.6}Mn_{16.7}Co_{16.7}$ alloy at 1393 K. The insets show an enlarged view of the second peak and the area of the prepeak: (*1*) the above ternary melt, (*2*) liquid Al, (*3*) Co, and (*4*) the liquid binary $Al_{76.5}Co_{23.5}$ alloy [27]. The dashed lines show SF generated by the RMC method.

maximum. The shortest interatomic distance for the liquid ternary $Al_{66.6}Mn_{16.7}Co_{16.7}$ alloy at 1393 K, which was obtained from the position of the first RDF peak, is 0.257±0.001 nm. Provided that this distance is 0.278 nm, 0.265 nm, and 0.246 nm for liquid Al, Mn, and Co respectively, we can speak about an intense interaction between the atoms in the ternary melt. The insets (Fig. 2) show the areas of the second peak and prepeak of the ternary melt in comparison with liquid Al and Co and the liquid binary $Al_{76.5}Co_{23.5}$ alloy. Note that liquid Al does not have the said SF features, liquid Co exhibits an asymmetric second peak, and the binary melt shows a prepeak only.

Thus, the obtained experimental SFs of liquid copper and the liquid ternary $Al_{66.6}Mn_{16.7}Co_{16.7}$ alloy show signs of the presence of structural features in these melts. To investigate the nature of these features, we performed a simulation of the melts and a detailed analysis of the structural models obtained.

STUDY OF THE POLYTETRAHEDRAL ORDER

Delaunay simplices were calculated for all the structural models. Formula (1) was used to find the values of T for the simplices and, hence, the number of quasi-perfect simplices converging in each atom, i.e., the number of quasi-perfect simplices for which this atom is a common vertex. At this stage we do not distinguish between the atoms in the melt. Figs. 3*a, b* show the distribution of the atoms by the number of quasi-perfect tetrahedra in their environment. First of all, we note that, in all our models, atoms bring together a relatively small number of quasi-perfect simplices around themselves. Only a small fraction of the atoms (less than 1%) have 10 or more simplices, and there are absolutely no atoms that would bring together 20 tetrahedra, as in the case of an icosahedral local environment. Thus, it can be an evidence of the absence of icosahedral environments in these melts; less compact clusters of quasi-perfect tetrahedra are present instead of them.

The greater the rightward shift of the distribution, the larger the number of tetrahedra in the system. We say that in this case the polytetrahedral order in the melt is stronger. Note that the display of the polytetrahedral order in the SF may depend not only on the number of quasi-perfect tetrahedra but also on how they are organized. This issue requires further study, and we plan to discuss it specifically in our next paper. Here we confine ourselves to a qualitative assessment of the polytetrahedral order by characterizing it with the distributions shown in Fig. 3*a, b*.

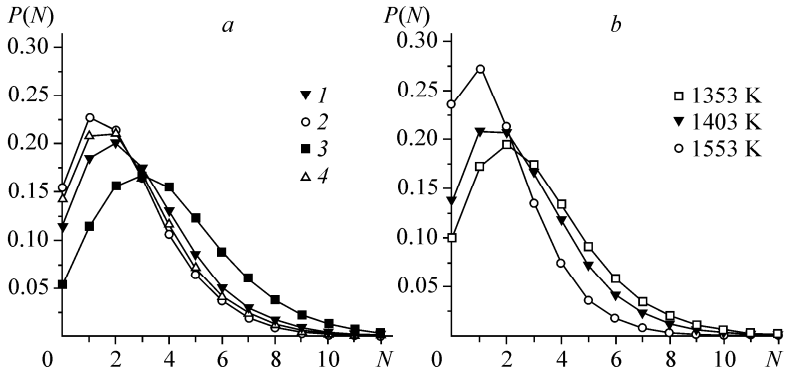

Fig. 3. Distribution of the number of quasi-perfect tetrahedra around the atoms (*a*) in the model melts: (*1*) $Al_{66.6}Mn_{16.7}Co_{16.7}$, (*2*) Al, (*3*) Co, and (*4*) $Al_{76.5}Co_{23.5}$ and (*b*) in the models of liquid copper at different temperatures.

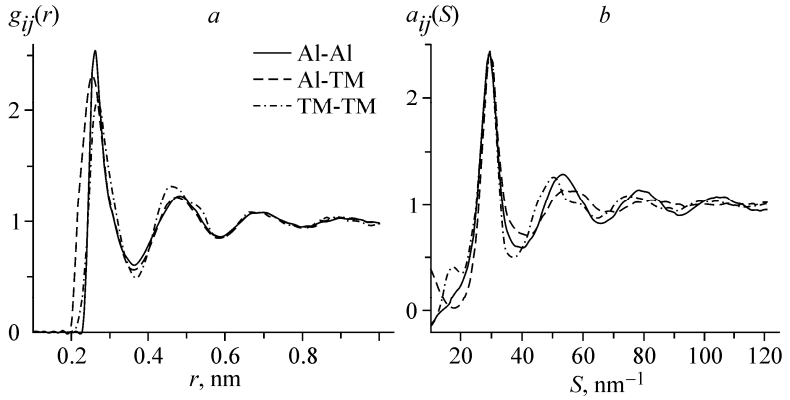

Fig. 4. Partial pair correlation functions (*a*) and structure factors (*b*) for the model of the liquid $Al_{66.6}Mn_{16.7}Co_{16.7}$ alloy. The Mn and Co atoms are considered as one type of atoms (TM).

Fig. 3*a* shows that the shift of the distributions towards a larger number of the tetrahedra correlates with the asymmetry of the second peak in SF (inset in Fig. 2). In particular, the ternary melt has a stronger polytetrahedral order than aluminum and the binary melt, which show practically no asymmetry of the second peak. Fig. 3*b* shows the change in the polytetrahedral order in liquid copper with temperature. The distribution is significantly shifted to the right and the asymmetry of the second peak increases with decreasing temperature (Fig. 1), which again points to a relation between the polytetrahedral order and the asymmetry of the second maximum.

STUDY OF CSRO IN ALUMINUM ALLOYS WITH TRANSITION METALS

The resulting structural models of $Al_{76.5}Co_{23.5}$ and $Al_{66.6}Mn_{16.7}Co_{16.7}$ were used to calculate the following partial characteristics: the partial SFs ($a_{ij}(S)$) and partial pair correlation functions ($g_{ij}(r)$). They are shown in Fig. 4 for the ternary melt, where the atoms Co and Mn are treated as one type (TM). The partial $g_{\mathrm{TMTM}}(r)$ is characterized by a higher second peak and, consequently, a lower first peak, compared to the curves $g_{\mathrm{AlTM}}(r)$ and $g_{\mathrm{AlAl}}(r)$ (Fig. 4*a*). This explicitly indicates that the TM atoms are pushed out into the second coordination sphere relative to each other, which is evidence of the existence of CSRO (deviation from the stoichiometric distribution of one component around another). This order is attributed to a more intense interaction between the atoms of Al and TM, which is discussed in [10, 27]. This is also evidenced by the calculated shortest interatomic distances: $R_1(i–j)$: R_1(Al–Al) =0.263 nm, R_1(Al–TM) = 0.251 nm, and R_1(TM–TM) = 0.268 nm.

The partial SF $a_{TMTM}(S)$ displays a sharp prepeak (Fig. 4*b*), which indicates the appearance of a characteristic length scale associated with the specific distribution of TM atoms relative to each other. This peak is manifest in the experimental SF because the aluminum and TM atoms have different scattering powers.

A quantitative characteristic of CSRO is the Warren–Cowley parameter α_p [32] calculated as a deviation of the local concentration of atoms from the stoichiometrical one

$$\alpha_p = 1 - \frac{z_{12}}{c_2\langle z\rangle} = 1 - \frac{z_{21}}{c_1\langle z\rangle}, \quad (2)$$

where c_i is the atomic concentration of the component i; z_{ij} is the coordination number of atoms j around atoms i; and $\langle z\rangle = c_2(z_{11} + z_{12}) + c_1(z_{21} + z_{22})$ is the average coordination number of the local environment of the atoms. The coordination numbers z_{ij} in the models were found as the number of atoms of type j around atoms of type i at a distance between R_1 (the maximum convergence between the atoms) and R_2 (the position of the first minimum in the curves $g_{ij}(R)$), which is averaged over all the i type atoms. A negative value of α_p indicates the prevailing coordination of atoms of one type around those of the other type. A positive value indicates the coordination of atoms of one type, and zero is the absence of CSRO. For our ternary melt, this value is –0.040. Previously, we calculated it for the liquid $Al_{76.5}Co_{23.5}$ alloy (α_p = –0.024) and for a model of the liquid ternary $Al_{71.6}Ni_{23}Fe_{5.4}$ alloy (α_p = –0.021) [14].

It should be noted that intermetallic Al_4MnCo, $Al_{13}Co_4$, and Al_5Fe_2 compounds, which correspond to the multicomponent melts in the study, exhibit a high degree of CSRO and an intense interaction between the atoms of Al and TM. One can say that the features of interatomic interactions that are typical of solids are retained during melting, which leads to the appearance of CSRO in the melt.

SIMULATION OF CHEMICAL ORDERING IN A HOMOGENEOUS SYSTEM

The RMC model of liquid aluminum was used to generate binary model systems $Al_{76.5}X_{23.5}$ with different degrees of CSRO. For this purpose, a part of Al atoms were renamed into atoms of another type, X. The selection of these Al atoms was mostly random but with a condition to reduce the probability of occurrence of X atoms in one another immediate environment. Thus, the probability of replacement of an Al atom by an X atom was calculated by the formula $p = 1/a^n$, where n is the number of X atoms that are already in the local environment of the Al atom. The parameter a defines the "strictness" of CSRO being modeled. Varying the values of a, we can change the fraction of X atoms in the immediate environment of X atoms. If a = 1, all X atoms are distributed randomly and there is no CSRO; however, at $a > 1$ it will necessarily appear. Note that the particular type of the formula to calculate the probability is not so important. It only matters whether the use of this procedure would reduce the number of X atoms in their local atomic environments and, consequently, increase the number of these atoms at longer distances.

Fig. 5*a* shows the partial pair correlation functions $g_{ij}(r)$ for a model generated by the above algorithm in the case when a = 2 and 23.5% of Al atoms are replaced by X atoms. The resulting situation is similar to the pattern of CSRO in the liquid $Al_{76.5}Co_{23.5}$ alloy investigated in [10]. One can see the expected change in the intensity ratio of the first and second peaks in $g_{ij}(r)$. Fig. 5*b* shows the partial structure factors $a_{ij}(s)$. The prepeak is visible in the curve $a_{XX}(s)$, displaying an analogy with the curve $a_{TMTM}(s)$ in Fig. 4*b*. Clearly, in the case of an identical scattering power of the Al and X atoms, no prepeak is observed in the total SF for the model melt, which is based on pure Al. However, if the X atoms are assigned a different (higher) scattering power, the prepeak will be visible in the total SF, as is the case of aluminum alloys with transition metals.

With the increase in the "strictness" of CSRO (increase in the parameter a), there is a noticeable strengthening of the second peak in the partial $g_{XX}(r)$ and the prepeak in $a_{XX}(s)$. The calculation of the Warren–Cowley parameter at a = 1, 1.5, 2, and 4 gives: α_p = 0, –0.056, –0.083, and –0.123, respectively. Note that this CSRO was obtained without changing the structure of the original system, which means that they can be manifest independently of each other.

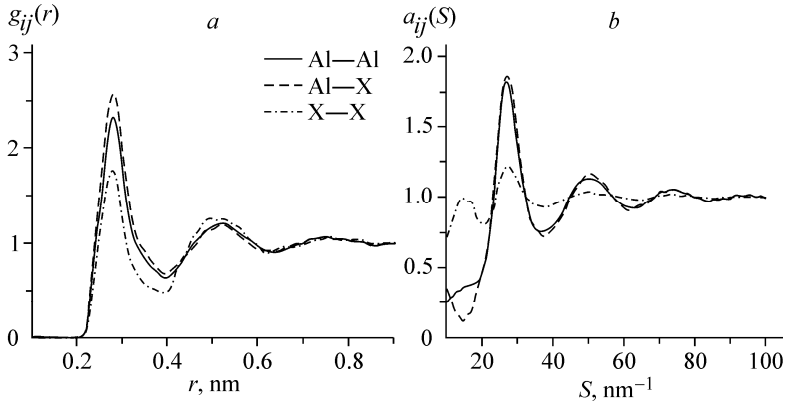

Fig. 5. Partial pair correlation functions (*a*) and structure factors (*b*) for the model binary system Al–X (the parameter $a = 2$, see text).

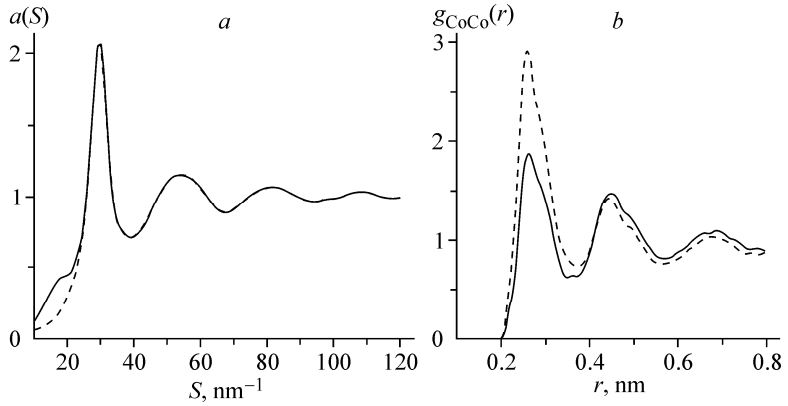

Fig. 6. Experimental structure factor for the liquid binary $Al_{76.5}Co_{23.5}$ alloy before (solid line) and after (dashed line) the artificial removal of the prepeak (*a*). Partial pair correlation function $g_{CoCo}(r)$ in the RMC models of the binary melt obtained in the presence (solid line) and absence (dashed line) of the prepeak (*b*).

ANALYSIS OF THE RELATIONSHIP BETWEEN THE POLYTETRAHEDRAL ORDER AND CSRO

In order to search for the structural features that are directly related to the prepeak, we built an artificial model of the liquid binary $Al_{76.5}Co_{23.5}$ alloy from the experimental curve of the structure factor from which we had removed the prepeak. The main peak and the prepeak in the intensity curve were approximated using the pseudo-Voigt function and the prepeak was subtracted from the total curve (Fig. 6). The resulting curve of the structure factor without the prepeak was used to build an RMC structural model of the binary melt.

An analysis of the model showed that the RDF of the melt remained almost unchanged after the removal of the prepeak. This means that the general arrangement of the atoms remained unchanged. In addition, we calculated the distribution of the atoms by the number of quasi-perfect simplices to find it to be almost identical to the one shown in Fig. 3, which was calculated with the prepeak. This might mean that the polytetrahedral order in our melt bears no relationship to the prepeak. However, there were significant changes in the partial functions. Fig. 6*b* shows the pair correlation functions. After the removal of the prepeak, the first peak of $g_{CoCo}(r)$ became as intense as the one in the total distribution function; i.e., the Co atoms in our artificial model are not pushed out into the second coordination sphere as in the presence of the prepeak. There is no prepeak in the partial structure factor $a_{CoCo}(S)$ either if the prepeak in the total SF is removed.

CONCLUSIONS

An X-ray diffraction study was performed of the liquid ternary $Al_{66.6}Mn_{16.7}Co_{16.7}$ alloy at 1393 K and liquid copper at 1353 K, 1403 K, and 1553 K. The structure factor curve of copper was shown to display the asymmetry of the second peak with decreasing temperature. The ternary melt exhibits both asymmetry of the second peak and prepeak. The reverse Monte Carlo (RMC) method was used to generate structural models of these melts and also of liquid Al and Co and the liquid binary $Al_{76.5}Co_{23.5}$ alloy.

A detailed analysis of the structural models clearly shows that the asymmetry of the second peak of SF is a result of the polytetrahedral order, i.e., is due to the existence in the melt of a noticeable amount of atomic configurations whose shape is close to a regular tetrahedron, which are combined into clusters of varying morphology. The reason for the prepeak is CSRO, i.e., the predominant location of some atoms in the immediate environment of other atoms. In this case, aluminum atoms prefer to be near transition metal atoms. This leads to the appearance in the solution of a characteristic length scale that is larger than the shortest interatomic distances, which is a precondition for the prepeak in SF. The simultaneous presence of both features in SF of aluminum alloys with transition metals is explained by the existence of the polytetrahedral order in the melt, but this order is accompanied by CSRO, which results in the presence of the prepeak owing to different scattering powers of the components.

This work was supported by RFBR project no. 10-03-90900, and also in part by RFBR project No. 12-03-654.

REFERENCES

1. D. M. Herlach, P. Galenko, and D. Holland-Moritz, *Metastable Solids from Undercooled Melts*, ISBN 0080436382 (0-08-043638-2), Hardcover, Elsevier (2007).
2. M. Maret, J. M. Dubois, and P. Chieux, *J. Non-Cryst. Solids*, **156-158**, 918 (1993).
3. S. R. Elliot, *J. Phys.: Condens. Matter*., **4**, No. 38, 7661 (1992).
4. M. Wilson and P. A. Madden, *Phys. Rev. Lett*., **80**, 532 (1998).
5. L. Yang, J. Z. Jiang, K. Saksl, et al., *J. Phys.: Condens. Matter*., **19**, No. 38, 476217 (2007).
6. V. P. Voloshin, S. Beaufils, and N. N. Medvedev, *J. Mol. Liq*., **101**, 96 (2002).
7. V. P. Voloshin and N. N. Medvedev, *J. Struct. Chem*., **46**, No. 1, 93 (2005).
8. O. Genser and J. Hafner, *J. Phys.: Condens. Matter*., **13**, No. 5, 981 (2001).
9. C. Bergman, K. Seifert-Lorenz, M. V. Coulet, et al., *Europhys. Lett*., **43**, No. 5, 539 (1998).
10. T. Schenk, V. Simonet, D. Holland-Moritz, et al., *Europhys. Lett*., **65**, No. 1, 34 (2004).
11. K. F. Kelton, A. K. Gangopadhyay, T. H. Kim, et al., *J. Non-Cryst. Sol*., **352**, 5318 (2006).
12. D. Holland-Moritz, T. Schenk, P. Convert, et al., *Meas. Sci. Technol*., **16**, 372 (2005).
13. F. C. Frank, *Proc. R. Soc. London A*, **215**, 43 (1952).
14. O. S. Roik, A. V. Anikeenko, and N. N. Medvedev, *J. Mol. Liq*., **161**, No. 2, 78 (2011).
15. D. R. Nelson and F. Spaepen, *Solid State Physics*, **42**, 1 (1989).
16. D. Holland-Moritz, T. Schenk, R. Bellissent, et al., *J. Non-Cryst. Sol*., **312-314**, 47 (2002).
17. D. Holland-Moritz, O. Heinen, R. Bellissent, et al., *Mat. Sci. Eng. A*, **449-451**, 42 (2007).
18. O. J. Eder, E. Erdpresser, B. Kunsch, et al., *J. Phys. F: Metal Phys*., **10**, No. 2, 183 (1980).
19. T. Roussel, C. Mottet, and C. Bichara, *J. Non-Cryst. Sol*., **353**, 3679 (2007).
20. L. Wang, Y. Wang, C. Peng, et al., *Phys. Lett. A*, **350**, 405 (2006).
21. V. Simonet, F. Hippert, H. Klein, et al., *Phys. Rev. B*, **58**, 6273 (1998).
22. M. Krajci and J. Hafner, *J. Phys.: Condens. Matter*., **14**, No. 30, 7201 (2002).
23. V. P. Kazimirov, V. È. Sokol'skii, A. S. Roik, and A. V. Samsonnikov, *Structure of Disordered Systems: Theory and Simulation* [in Russian], Kievskii Universitet, Kyiv (2009).

24. W. Bol, *J. Sci. Instr*., **44**, No. 9, 736 (1967).
25. A. A. Katznelson (ed.), in: *X-Ray Diffraction. Special Practical Course* [in Russian], Izd. MGU., Moscow (1986).
26. R. L. MacGreevy, *J. Phys. Condens. Matter*., **13**, R877 (2001).
27. O. S. Roik, O. V. Samsonnikov, V. P. Kazimirov, et al., *J. Mol. Liq*., **145**, 129 (2009).
28. N. N. Medvedev, *The Voronoi–Delaunay Method in the Study of the Structure of Noncrystalline Systems* [in Russian], SO RAN NITs OIGGM, Novosibirsk (2000).
29. J. D. Bernal, *Proc. R. Soc. London A*, **280**, 299 (1964).
30. Y. I. Naberukhin, V. P. Voloshin, and N. N. Medvedev, *Mol. Phys*., **73**, 917 (1991).
31. H. Jonsson and H. Andersen, *Phys. Rev. Lett*., **60**, 2295 (1988).
32. *Novel Application of Anomalous* (*Resonance*) *X-Ray Scattering for Structural Characterization of Disordered Materials*, Springer Berlin, Heidelberg, Vol. 204 (1984) (DOI 10.1007/BFb0025745, ISBN978-3-540-13359-9).